Numerical Methods in Civil Engineering

Pseudo-spectral method for mechanical buckling analysis of circular plates with variable thickness made of bimorph FGMs

Hossein Khosravi*, Mahmood Khosravi**, Mojtaba Lezgy-Nazargah***

ARTICLE INFO

Article history:
Received:
August 2018.
Revised:
November 2018.
Accepted:
December 2018.

Keywords:
Mechanical buckling
Circular plate
Variable thickness
Functionally graded materials
Pseudo-spectral method

Abstract:

In this paper, the mechanical buckling behavior of circular plates with variable thicknesses made of bimorph functionally graded materials (FGMs) under uniform mechanical loading circumstances has been studied for the first time. The governing equations are derived based on the first-order shear deformation plate theory and von Karman's assumptions. The material characteristics are symmetric about the middle plane of the plate and these characteristics vary along the thickness direction according to the power law. The middle plane of the plate is made of pure metal, which changes to pure ceramic as it approaches the outer sides. In order to determine the pre-buckling force in the radial direction, the membrane equation is solved using the shooting method. Then, the stability equations are solved numerically with the help of pseudo-spectral method and choosing the Chebyshev polynomials as basis functions. The numerical results are presented for both clamped and simply supported boundary conditions by considering linear and parabolic patterns for the thickness variations. The influences of various parameters like volume fraction index, thickness profile and side ratio on the buckling behavior of these plates have been evaluated. The obtained numerical results show that there exists an optimal value for the thickness parameter, wherein the buckling load becomes maximum. The buckling load of circular FGM plates increases more than 100% when the volume fraction index increases from 0 to 5. The buckling load of the clamped circular FGM plates decreases about 15% as the side ratio increases from 0.01 to 0.2.

1. Introduction

The plates are very important structural elements due to the fact that they can be fabricated in different geometrical shapes and furthermore, they are also being utilized in various industries. Based on their usage, thermal or mechanical buckling may occur in the plates. Applying unallowable mechanical loads to the plates may damage them or make them unstable. Hence, the investigation of the plate's stability behavior should be regarded as an important issue in engineering discipline. In the engineering computations and designations, the determination of the minimum buckling load is a key issue.

*Assistant Professor, Department of Civil Engineering, Hakim Sabzevari University, Sabzevar, Iran
** Corresponding Author: Ph.D. Student, Department of Mechanical Engineering, Faculty of Engineering, Islamic Azad University, South Tehran Branch, Tehran, Iran. Email: mahmod.khosravi@yahoo.com
***Associate Professor, Department of Civil Engineering, Hakim Sabzevari University, Sabzevar, Iran

During the recent years, functionally graded materials have been used in advanced professions, especially in the space and nuclear industries. Until now, a large number of researches have been conducted on these materials. The FGMs are usually made of a mixture of ceramic and metal or a combination of ceramic, metal and other alloys. From micro-structural point of view, these materials are non-homogenous and their micro-structural properties, including the distribution type and the phase size, alter in a continuous and smooth manner. These gradual changes of the micro-structural properties lead to the gradual changes of the thermal and mechanical properties in FGMs [1]. The plate type structural elements of FGMs have their wide applications in nuclear energy reactors, solar energy generators and space shuttles. They have also particular applications in industries related to defense. For example, FGM plates are used as penetration resistant materials for armour plates and bullet-proof vests [2].

One of the important and hot topics related to the solid mechanics is the stability analysis and the investigation of the buckling behavior of the plates. Moreover, designers have always paid heed to the plates

with variable thickness, whenever they aimed to satisfy the economic considerations. It was in 1891, that Brayan [3] proposed the first solution for the stability problem of the plates. He investigated the buckling of a circular plate with clamped boundary conditions under a radial uniform load. Another research was carried out by Yamaki [4] who focused on the buckling of annular plates. In this reference, the mechanical loads were applied on the internal and external edges of the annular plate. Yamaki showed that the critical buckling mode of the annular plates is usually different from the corresponding critical buckling mode of the circular plates. Another study was carried out by Timoshenko and Gere [5]. They concentrated on the stability problem of various engineering structures such as columns, frames, curved beams, plates and membranes. Then, Brush and Almroth [6] comprehensively analyzed the buckling problems of columns, plates and membranes. They derived formulations related to the non-linear equilibrium and stability equations of the aforementioned structures. Reddy and Khdeir [7] have focused on the buckling and free vibration analysis of the multi-layer composite rectangular plates with various boundary conditions by using classic, first-order and third-order shear deformation theories. In addition to the analytic solution, the numerical solution was also provided based on the finite element method (FEM). Kadkhodayan et al. [8] investigated the buckling analysis of circular, annular and rectangular plates based on the classic theory. They used the dynamic relaxation method for solving the governing equations. The obtained results of these researchers indicate that the classic theory estimates the natural frequencies and critical knuckling loads beyond the actual values. They showed that this difference increases by increasing the thickness to the lateral length ratio. Based on the first-order shear deformation theory and by using the FEM, Ozakca et al. [9] studied the buckling behavior and optimum design of the variable thickness circular and annular plates. Xu et al. [10] used three-dimensional (3D) thermal elasticity for the mechanical buckling analysis of the circular and annular plates. They obtained results for various distributions of the Poisson's ratio and made a comparison between them. Najafizadeh and Eslami [11, 12] investigated the buckling analysis of circular plates made of one-sided functionally graded materials under various types of thermal loading and boundary conditions. They used the classic theory and presented an analytical solution for the plates under the uniform radial compression. Naei et al. [13] studied the mechanical buckling of variable thickness circular plates made of one-sided FGMs under uniform radial pressure based on FEM and the classical plate theory. In their research, they considered both simply supported and clamped boundary conditions. Based on the first-order shear deformation theory, Sepahi et al. [14] investigated the thermal buckling and post-buckling analysis of the annular plates made of FGMs. They assumed a particular pattern of distribution for variations of the temperature along the radial direction. They solved the governing differential equations by using the differential quadrature method. Golmakani and Emami [15] studied the non-linear bending and buckling analysis of the annular plates made of FGMs. They assumed a special distribution for the FGMs along the radial direction. In this reference, the numerical solution is based on the dynamic release method and the governing equations are extracted based on the first-order shear deformation theory. Khosravi and colleagues [16, 17] presented a precise closed-form solution for the thermal buckling of circular plates made of bimorph FGMs by adopting the first-order shear deformation theory. They evaluated the effects of different factors including the ratio of thickness to the plate radius and the volume fraction index on the critical temperature. Lezgy-Nazargah et al. [18] investigated the static, free vibration and dynamic responses of beams made of functionally graded piezoelectric material via an efficient three-noded beam element. The FEM of these researchers is based on a refined trigonometric shear deformation theory which does not need any shear correction factor. Lezgy-Nazargah and Farahbakhsh [19] studied the relation between the material gradient properties and the optimum sensing/actuation design of the functionally graded piezoelectric beams. They used 3D finite element analysis in order to find an optimum composition profile for these types of sensors and actuators. A 3D exact solution was presented by Lezgy-Nazargah for cylindrical bending and dynamic free vibration analyses of the functionally graded piezoelectric laminated plates [20, 21]. Lezgy-Nazargah solved the exact 3D equilibrium equations by using the Peano series solution and adopting the state space formalism. Lezgy-Nazargah [22] studied the fully coupled thermo-mechanical behavior of bi-directional FGM beams by adopting a computationally low cost isogeometric FEM. For presenting the in-plane displacement field, Lezgy-Nazargah used a combination of polynomial and exponential expressions. Lezgy-Nazargah and Meshkani [23] developed a four-node quadrilateral partial mixed plate element with low degrees of freedom for static and free vibration analyses of FGM plates rested on Winkler-Pasternak elastic foundations. They obtained the discrete form of the governing equations by employing the partial form of the Reissner's Mixed Variational Theorem. By using the first-order shear deformation theory, Baferani et al. [24] studied the free vibration response of FGM rectangular plates. They investigated the effects of in-plane displacements on the natural frequencies of such plates. Based on the power series expansions, Soltani [25] developed a semi-analytical technique to investigate the free bending vibration behavior of axially functionally graded non-prismatic Timoshenko beams subjected to a point force at both ends. In this reference, the exact fundamental solutions are acquired by expressing the variable coefficients that appeared in motion equations in a polynomial form. Stability analysis of thin-walled beams and columns was also studied by Soltani and colleagues [26-29].

In this study, the first-order shear deformation theory and von Karman's assumptions were utilized for the mechanical buckling analysis of circular plates with variable thickness. It is assumed that the plate is made of the bimorph FGMs. For obtaining the equilibrium

equations, the stationary potential energy method is utilized. The equilibrium equations are firstly obtained via the adjacent equilibrium method. Then, the equilibrium equations are solved by employing the pseudo-spectral method by selecting the Chebyshev polynomials as the basis functions. Note that pseudo-spectral methods are a class of numerical methods used in applied mathematics and scientific computing for the solution of partial differential equations. These methods are also known as discrete variable representation methods. They are closely related to spectral methods, but complement the basis with an additional pseudo-spectral basis, which allows representation of functions on a quadrature grid [30]. The effects of geometric parameters, material properties and mechanical loading on the buckling behavior are discussed in details for the plates with both simply supported and clamped boundary conditions. For validation, the results were compared with previous published works. The comparisons show that the results predicted by the present formulation are extremely accurate.

2. Governing equations of the problem

2.1. Plates with variable thickness

In FGM plates, the mechanical properties usually change in the thickness direction depending on the volume fraction of the constituent elements. Variations of the volume fraction at any point along the thickness direction are dependent to the distance of that point from the reference plane as well as the thickness size of the plate. Assume a circular FGMs plate in the cylindrical coordinate system (r,θ,z). In this system, r, θ and z represent the radial, circumferential and thickness directions, respectively. If the plate thickness is constant, then the volume fraction will be the same for all sections and it will only be a function of the z coordinate. However, if the plate thickness is variable, the thickness size will be different in the radial direction, which will make the definition of the volume fraction more complex. With regard to the model used for defining the volume fraction, it is possible to consider two types of plates with variable thickness which are exceedingly different from each other, especially in terms of the production process. In the first model, the volume fraction variations are dependent on the thickness size. Since the thickness size in this model is variable in the r direction, so the volume fraction will be a function of both the r and z coordinates (see Fig. 1-a and Fig. 1-c). For the fabrication of such a plate according to powder metallurgy, it is essential to control and observe the ceramic and metal combination in both thickness and in-plane directions simultaneously. Another model can also be suggested for FGM plates with variable thickness. In this model, the volume fraction in the thickness direction is the same for all planes whose distances are equal from a reference plane. In other words, the volume fraction at a certain distance from the reference plane will be equal for all transverse sections. After reaching the second constituent material, the residual thickness of the plate is filled homogenously with second material. As shown in Fig. 1-b and Fig. 1-d, such distribution of the volume fraction leads to the development of a FGM layer with constant thickness. For the production of these types of FGM plates with variable thickness, it is essential to control the volume fraction values with respect to the reference plane only in the thickness direction. Therefore, the fabrication process of these types of FGM plates is similar to the production process of the FGM plates with constant thickness, which is not difficult to accomplish. One-sided, as well as bimorph FGM plates are illustrated in Fig. 1 based on the two possible models described for the volume fraction variation. The plate which is studied in this research is a bimorph FGM plate (see Fig. 1-c).

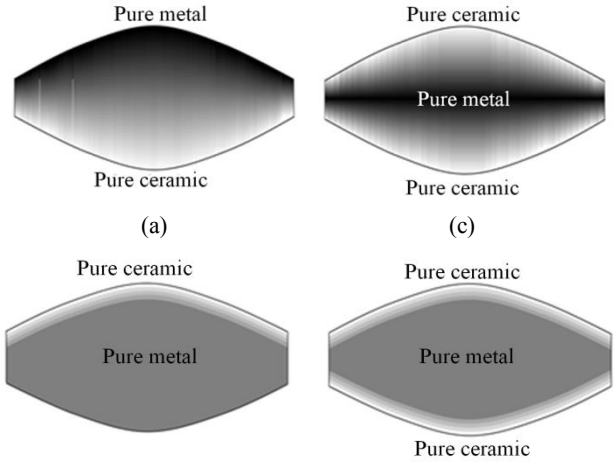

Fig. 1: Various types of circular plates with variable thickness: (a) one-sided FGM plate with volume fraction dependent on thickness; (b) one-sided FGM plate with a FGM layer of constant thickness; (c) bimorph FGM plate with volume fraction dependent on thickness; (d) bimorph FGM plate with a FGM layer of constant thickness

2.2. Problem Geometry

The geometry of the studied problem is an axially symmetric circular plate with radius b and thickness $h(r)$. As shown in Fig. 2, the coordinate system is located at the center of the plate upon the middle plane, and the r and z coordinates are located in the radial and thickness directions, respectively. Due to the axial symmetry, the circumference direction is not considered in the formulations.

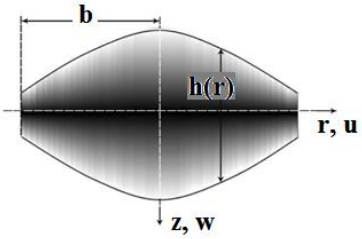

Fig. 2: Geometry of the circular bimorph FGM plate with variable thickness

The letters u and w indicate the displacements of the middle plane along the radial and thickness directions,

respectively. The total thickness of the plate $h(r)$ will be a function of the radial coordinate:

$$h(r) = h_1 + (h_2 - h_1)\left(\frac{r}{b}\right)^p \quad (1)$$

where h_1 and h_2 indicate the thickness of the plate at the center and edge, respectively. The profile variation of the thickness is showed by p parameter. Although the formulation and the method of solution allow the selection of any desirable value for the p parameter, the present solution is only accomplished for the linear and parabolic cases. p is assumed to be equal to 1 and 2 for the linear and parabolic case, respectively.

For a plate with the constant volume of V, the following relation is established between the geometric parameters:

$$h_0 = \frac{V}{\pi b^2} = h_1 + \frac{2(h_2 - h_1)}{p+2} \quad (2)$$

in which h_0 denotes the thickness of a plate with constant thickness and the same volume. Moreover, the variations of the thickness in the radial direction can be expressed by introducing the dimensionless taper parameter Ω:

$$\Omega = \frac{h_2}{h_1 + h_2} \quad (3)$$

The above parameter can be variable between 0 to 1. The zero value implies the maximum thickness at the center and zero thickness on the edge, while the 1 value indicates the maximum thickness on the edge and zero thickness at the center. The Ω=0.5 value implies a plate with constant thickness.

2.3 The governing equations of bimorph FGMs

The functionally graded materials are categorized as heterogeneous materials and the corresponding properties are a function of the volume fraction of constituent materials (i.e. ceramic and metal). Thus, the modulus of elasticity of FGMs can be written as:

$$E_f = V_m E_m + V_c E_c \quad (4)$$

where V_m and V_c are the volume fraction of the metal and ceramic, respectively. V_m and V_c can be defined as follows:

$$V_m = \left(\frac{2z + h(r)}{h(r)}\right)^N \qquad -\frac{h(r)}{2} \le z \le 0$$

$$V_m = \left(\frac{-2z + h(r)}{h(r)}\right)^N \qquad 0 \le z \le \frac{h(r)}{2} \quad (5)$$

$$V_c = 1 - V_m$$

N is the volume fraction index of the bimorph FGMs, which specifies the combination mode of the ceramic and metal volume fraction along the thickness direction. The zero and infinitive values for this index indicate the pure metal and ceramic, respectively.

2.4 Equilibrium and stability equations

According to the first-order shear deformation plate theory, the displacement field of the bimorph FGMs plate can be defined as follows:

$$\begin{aligned} U(r, z) &= u(r) + z\,\phi(r) \\ W(r, z) &= w(r) \end{aligned} \quad (6)$$

where $u(r)$ and $w(r)$ are displacements of the middle plane of the circular plate along r and z directions, respectively. $\phi(r)$ denotes the slope rotation in the r-z plane. The buckling problem is classified as the geometric nonlinear problem. By using Eq. (6), the strain-displacement equations can be defined as follows based on the von Karman's assumptions:

$$\begin{aligned} &\varepsilon_r = \varepsilon_{r0} + k_r z, \quad \varepsilon_\theta = \varepsilon_{\theta 0} + k_\theta z, \\ &\gamma_{rz} = \phi + w_{,r} \end{aligned} \quad (7)$$

The strain components can be expressed as follows:

$$\varepsilon_{r0} = u_{,r} + \frac{1}{2}(w_{,r})^2, \quad \varepsilon_{\theta 0} = \frac{u}{r} \quad (8)$$

The curvatures can also be expressed as follows:

$$k_r = \phi_{,r}, \quad k_\theta = \frac{\phi}{r} \quad (9)$$

in which $(\ )_{,r}$ denotes the derivative with respect to the radial coordinate. Given the fact that FGMs are isotropic materials, the stress-strain relations based on the Hooke's law can be expressed as follows:

$$\begin{aligned} \sigma_r &= \frac{E}{1-\nu^2}(\varepsilon_r + \nu\varepsilon_\theta) \\ \sigma_\theta &= \frac{E}{1-\nu^2}(\varepsilon_\theta + \nu\varepsilon_r) \\ \tau_{rz} &= \frac{E}{2(1+\nu)}\gamma_{rz} \end{aligned} \quad (10)$$

Note that the above equation is obtained by assuming a constant value for the Poisson's ratio and ignoring the stretching of the plate along the thickness direction. σ_θ and σ_r denote the in-plane normal stresses while τ_{rz} denotes the in-plane shear stress at a point with distance z from the mid-plane of the FGMs plate. By integrating the stress components over the thickness of the plate, the following expressions are obtained for the resultant forces and moments:

$$\begin{aligned} (N_r, N_\theta) &= \int_{-h(r)/2}^{h(r)/2} (\sigma_r, \sigma_\theta)\, dz \\ (M_r, M_\theta) &= \int_{-h(r)/2}^{h(r)/2} (\sigma_r, \sigma_\theta)\, z\, dz \\ Q_r &= K \int_{-h(r)/2}^{h(r)/2} \tau_{rz}\, dz \end{aligned} \quad (11)$$

K indicates the shear correction coefficient of the first-order shear deformation theory, and its value is taken as 5/6. By substituting Eq. (10) into Eq. (11), the relation between the resultant forces and moments in terms of the strain components can be calculated as:

$$\begin{pmatrix} N_r \\ N_\theta \end{pmatrix} = A_{11} \begin{bmatrix} 1 & \nu \\ \nu & 1 \end{bmatrix} \begin{pmatrix} \varepsilon_{r0} \\ \varepsilon_{\theta 0} \end{pmatrix}$$
$$\begin{pmatrix} M_r \\ M_\theta \end{pmatrix} = D_{11} \begin{bmatrix} 1 & \nu \\ \nu & 1 \end{bmatrix} \begin{pmatrix} \varepsilon_{r1} \\ \varepsilon_{\theta 1} \end{pmatrix} \quad (12)$$
$$Q_r = A_{55}\ \gamma_{rz}$$

Coefficients A_{11} and D_{11} are obtained by integrating the mechanical properties through the thickness of the plate. As the plate thickness is variable, the integration limits are a function of the radial coordinate. Thus, A_{11} and D_{11} coefficients will also be a function of the radial coordinate:

$$\left(A_{11}, D_{11}\right) = \int_{-h(r)/2}^{h(r)/2} \left(1, z^2\right) \frac{E(z)}{1-\nu^2}\, dz$$
$$A_{55} = K\, \frac{A_{11}(1-\nu)}{2} \quad (13)$$

The equilibrium equations for circular plates can be obtained by utilizing the principle of minimum potential energy, or directly by writing the equilibrium equations for one arbitrary element. Due to the axial symmetry, there exists no variation in the circumferential direction, and only the derivatives relative to the radial direction are present in the differential equations:

$$N_{r,r} + \frac{N_r - N_\theta}{r} = 0$$
$$Q_r + r\,Q_{r,r} + \left(r\,N_r\,w_{,r}\right)_{,r} = 0 \quad (14)$$
$$M_{r,r} + \frac{M_r - M_\theta}{r} - Q_r = 0$$

The equilibrium equation can be rewritten in terms of displacement components by employing the force-displacement and moment-displacement relations. By substituting relations (7), (9) and (12) into Eq. (14), we have:

$$A_{11}\,w_{,r}\,w_{,rr} + \frac{1}{2r}\left(A_{11}(1-\nu) + r\,A_{11,r}\right) w_{,r}^2 +$$
$$A_{11}\,u_{,rr} + \frac{1}{r}\left(A_{11} + r\,A_{11,r}\right) u_{,r} + \frac{1}{r}\left(\nu\,A_{11,r} - \frac{A_{11}}{r}\right) u = 0$$
$$w_{,rr}\left\{A_{55} + A_{11}\left(u_{,r} + \frac{3}{2}\left(w_{,r}\right)^2 + \nu\frac{u}{r}\right)\right\}$$
$$+ w_{,r}\left\{A_{55,r} + \frac{A_{55}}{r} + \left[\frac{A_{11}}{r}(1+\nu) + A_{11,r}\right] u_{,r}\right.$$
$$+ \frac{1}{2r}\left(A_{11} + r\,A_{11,r}\right)\left(w_{,r}\right)^2 + \nu\,A_{11,r}\,\frac{u}{r}$$
$$\left. + A_{11}\,u_{,rr}\right\} + A_{55}\,\varphi_{,r} + \left(A_{55,r} + \frac{A_{55}}{r}\right)\varphi = 0$$
$$D_{11}\,\varphi_{,rr} + \frac{1}{r}\left(D_{11} + r\,D_{11,r}\right)\varphi_{,r}$$
$$- \frac{1}{r}\left(\frac{D_{11}}{r} - \nu\,D_{11,r} + r\,A_{55}\right)\varphi - A_{55}\,w_{,r} = 0 \quad (15)$$

The above obtained equations are regarded as the non-linear system of differential equations. It is common to use the adjacent equilibrium method for obtaining the stability equations from non-linear equilibrium equations. This method is helpful for stability analysis of structures and calculating their critical buckling loads. This method works based on definitions of the first and second equilibrium paths and the bifurcation point. Using this method, the bifurcation points can be obtained from the solution of linear differential equations. The required equations of this method are extracted via perturbation technique, wherein the displacement field (u,w,ϕ) is replaced by the field ($u_0+u_1, w_0+w_1, \phi_0+\phi_1$). The initial equilibrium state (i.e. before buckling) is indicated by (u_0, w_0, ϕ_0), which refers to an equilibrium mode on the initial path and (u_1, w_1, ϕ_1) is infinitesimal displacements within the displacement field. It should be noted that, at the prebuckling state, the plate has not been buckled and the lateral displacement has not occurred, so w_0 and ϕ_0 are equal to zero.

By substituting these new fields into Eq. (15), all expressions which do not include infinitesimal displacements, will be excluded for the resulted equations. Furthermore, if the increase in the displacement is adequately small, only the first-order expressions of (u_1, w_1, ϕ_1) will remain in the equations, while other expressions with higher order expressions will be omitted. Hence, the resulted stability equations are linear and homogenous in terms of hypothetical small displacement fields. Therefore, the stability equations may be written as follows:

$$A_{11}\,u_{1,rr} + \frac{1}{r}\left(A_{11} + r\,A_{11,r}\right) u_{1,r} - \frac{1}{r^2}\left(A_{11} - \nu\,r\,A_{11,r}\right) u_1 = 0$$
$$\left(A_{55} + N_{r0}\right) w_{1,rr} + \frac{1}{r}\left[A_{55} + N_{r0} + r\left(A_{55,r} + N_{r0,r}\right)\right] w_{1,r}$$
$$+ A_{55}\,\phi_{1,r} + \frac{1}{r}\left(A_{55} + r\,A_{55,r}\right)\phi_1 = 0$$
$$D_{11}\,\phi_{1,rr} + \frac{1}{r}\left(D_{11} + r\,D_{11,r}\right)\phi_{1,r}$$
$$- \frac{1}{r^2}\left(D_{11} - \nu\,r\,D_{11,r} + r^2\,A_{55}\right)\phi_1 - A_{55}\,w_{1,r} = 0 \quad (16)$$

It is essential to noted that, finding a solution for this system will lead to finding an adjacent equilibrium state for the initial equilibrium state. The independent variables of this system are (u_1, w_1, ϕ_1). N_{r0} denotes the radial pre-buckling force. It can be observed that the first equation of the stability equations system is not dependent on the second and third equations. Therefore, the second and third equations will be used to determine the critical buckling compression. After solving the eigenvalue problem, the lowest value obtained for N_{r0} should be regarded as the critical buckling compression.

The pre-buckling mode is considered as the equilibrium state prior to the buckling occurrence and it can be determined via non-linear equilibrium of Eq. (15). However, it is worth taking into account that the plate has not experienced any flexural deformation in the pre-buckling state, and the value of w_0 and ϕ_0 is equal to zero. Concerning these conditions, the equilibrium equations should be rewritten as follows:

$$A_{11}u_{0,rr}+\frac{1}{r}\left(A_{11}+r\,A_{11,r}\right)u_{0,r}$$

$$-\frac{1}{r^2}\left(A_{11}-\nu\,r\,A_{11,r}\right)u_0=0 \tag{17}$$

The above equation is called the membrane equation of the plate, which is a simple linear differential equation. The only independent variable of the equation is u_0. By obtaining the value of u_0, the in-plane forces can be calculated as follows:

$$\begin{pmatrix}N_{r0}\\N_{\theta 0}\end{pmatrix}=A_{11}\begin{bmatrix}1 & \nu\\ \nu & 1\end{bmatrix}\begin{pmatrix}u_{0,r}\\ \dfrac{u_0}{r}\end{pmatrix} \tag{18}$$

The mechanical loading is in the form of uniform mechanical compression P, which is applied on the edge of the FGMs plate. In this case, the edge has more freedom to move in the radial direction. Due to the symmetry, the in-plane displacement at the center of the plate equals to zero. Hence, the boundary conditions of the membrane equation are as follows:

$u_0(0)=0$ (at center)

$$N_{r0}=A_{11}\left(u_{0,r}+\frac{\nu}{b}u_0\right)=-P \quad \text{(on edge)} \tag{19}$$

Furthermore, in order to solve the stability Eq. (16), it is essential to determine the boundary conditions for lateral displacement and rotation at the center and on the edge of the circular FGMs plate. Two different boundary conditions are assumed for the edge of the circular plate: simply supported and clamped. Thus, the boundary conditions of the stability equations are as follows:

$\phi_1(0)=0, w_{1,r}(0)=0$ (at center)

$w_1(b)=0, \phi_1(b)=0$ (clamped edge)

$$\begin{cases} w_1(b)=0\\ \phi_{1,r}(b)+\dfrac{\nu}{b}\phi_1(b)=0\end{cases} \quad \text{(simply supported edge)} \tag{20}$$

3. Solving Numerical Equations

3.1. Solving membrane equation

Numerical integration methods can be employed to solve simple differential equations with variable coefficients; the most conventional one is Runge-Kutta method. However, the application of these methods is limited, and they can be used only for solving initial value problems. The boundary value problem can be converted into initial value problem using the shooting method, and then one can utilize conventional methods and simple numerical integrations (e.g. Runge-Kutta method) to solve the problem. The membrane Eq. (17) is regarded as a second-order simple linear differential equation, and by solving it, the value of in-plane displacement (u_0) and its derivative ($u_{0,r}$) will be obtained. The equation may be solved using the fourth-order Runge-Kutta method. Using the force-displacement relations, the in-plane radial force, which is taken into account as the pre-buckling load can be calculated.

3.2. Solving stability equations

The pseudo-spectral approaches are regarded as a family of methods used for solving differential equations. The fundamental idea of this method is the approximation of unknown function $u(x)$ by superposition of (n+1) sentence of basis functions $\zeta_j(x)$ with unknown amplitude a_j [30]:

$$u(x)\approx\tilde{u}(x)=\sum_{j=1}^{n+1}a_j\,\zeta_j(x) \tag{21}$$

The selection of base functions for any problem should be accomplished with considering the problem geometry. Although various types of base functions can be used in the pseudo-spectral method, Chebyshev polynomials are the most important and significant functions that are helpful for non-oscillating problems with a limited geometry. The simplest method for obtaining these basis functions is using the following recursive relations:

$$T_1=1$$
$$T_2=x$$
$$T_{n+1}=2x\,T_n-T_{n-1} \tag{22}$$

In the other words, we have taken $\zeta_j(x)=T_j(x)$ to solve the plate's differential equations by using the pseudo-spectral approach. The details of the pseudo-spectral method can be found in Boyd's book [30].

In order to solve the equations related to the FGM plates using pseudo-spectral methods, the stability equations and boundary conditions should be transmitted from the physical range of $r\in[0,b]$ to the solution range of $x\in[-1,1]$ as:

$$x=\frac{2r}{b}-1, \qquad dx=\frac{2}{b}dr \tag{23}$$

We also introduce the following dimensionless values:

$$x_1=\frac{w_1}{b},\ x_2=\phi_1,\ \bar{N}_{r0}=\frac{N_{r0}}{A_{55}}$$
$$\bar{N}'_{r0}=\frac{b\,N_{r0,r}}{2A_{55}},\ \bar{A}'_{55}=\frac{b\,A_{55,r}}{2A_{55}} \tag{24}$$
$$\bar{D}'_{11}=\frac{b\,D_{11,r}}{2D_{11}},\ \bar{F}=\frac{b^2A_{55}}{D_{11}}$$

By using Eqs. (23) and (24), the dimensionless stability equations and corresponding boundary conditions can be rewritten as follows:

$$2\left(\bar{N}_{r0}+1\right)x_1''+2\left[\frac{\left(\bar{N}_{r0}+1\right)}{(x+1)}+\left(\bar{A}'_{55}+\bar{N}'_{r0}\right)\right]x_1'$$
$$+x_2'+\left[\frac{1}{(x+1)}+\bar{A}'_{55}\right]x_2=0$$

$$2x_2'' + 2\left[\frac{1}{(x+1)} + \bar{D}_{11}'\right]x_2'$$
$$-2\left[\frac{1}{(x+1)^2} - \frac{\nu\bar{D}_{11}'}{(x+1)} + \frac{\bar{F}}{4}\right]x_2 - \bar{F}\,x_1' = 0 \qquad (25)$$

$x_1'(-1) = 0, x_2(-1) = 0$ (at center)
$x_1(1) = 0,\ x_2(1) = 0$ (clamped edge)
$$\begin{cases} x_1(1) = 0 \\ x_2'(1) + \dfrac{\nu}{2}x_2(1) = 0 \end{cases}$$ (simply supported edge) (26)

Note that $(\ )'$ indicates the derivative with respect to x variable. The independent variables of the stability equations are x_1 (dimensionless transverse displacement) and x_2 (rotation in the r-z plane). In the pseudo-spectral method, the solution is regarded as a set of Chebyshev's basis functions. As a result, the x_1 and x_2 variables at the i-th collocation point are considered as follows:

$$x_{1i} = \sum_{j=1}^{n+1} a_j T_{i,j}$$
$$x_{2i} = \sum_{j=1}^{n+1} b_j T_{i,j} \qquad (27)$$

The subscript j refers to j-th Chebyshev polynomial while the superscript i refers to the i-th collocation point. By substituting the above mentioned equations into the stability Eq. (25), the following equations in terms of Chebyshev's basis functions will be obtained:

$$2\left(\bar{N}_{r0}+1\right)\sum_{j=1}^{n+1} a_j T_{i,j}''$$
$$+2\left[\frac{\left(\bar{N}_{r0}+1\right)}{(x+1)} + \left(\bar{A}_{55}' + \bar{N}_{r0}'\right)\right]\sum_{j=1}^{n+1} a_j T_{i,j}'$$
$$+\sum_{j=1}^{n+1} b_j T_{i,j}' + \left[\frac{1}{(x+1)} + \bar{A}_{55}'\right]\sum_{j=1}^{n+1} b_j T_{i,j} = 0$$
$$2\sum_{j=1}^{n+1} b_j T_{i,j}'' + 2\left[\frac{1}{(x+1)} + \bar{D}_{11}'\right]\sum_{j=1}^{n+1} b_j T_{i,j}'$$
$$-2\left[\frac{1}{(x+1)^2} - \frac{\nu\bar{D}_{11}'}{(x+1)} + \frac{\bar{F}}{4}\right]\sum_{j=1}^{n+1} b_j T_{i,j}$$
$$-\bar{F}\sum_{j=1}^{n+1} a_j T_{i,j}' = 0 \qquad (28)$$

Similarly, the following equations will be obtained for the boundary conditions:

$$\begin{cases} \sum_{j=1}^{n+1} a_j T_{1,j}' = 0 \\ \sum_{j=1}^{n+1} b_j T_{1,j} = 0 \end{cases}$$ (at center)

$$\begin{cases} \sum_{j=1}^{n+1} a_j T_{n+1,j} = 0 \\ \sum_{j=1}^{n+1} b_j T_{n+1,j} = 0 \end{cases}$$ (clamped edge)

$$\begin{cases} \sum_{j=1}^{n+1} a_j T_{n+1,j} = 0 \\ \sum_{j=1}^{n+1} b_j T_{n+1,j}' \\ +\dfrac{\nu}{2}\sum_{j=1}^{n+1} b_j T_{n+1,j} = 0 \end{cases}$$ (simply support edge) (29)

Concerning the fact that there are two independent variables, we need (2n+2) algebraic equation for solving the problem. The equations linked to the boundary conditions (29) can supply four algebraic equations. Finally, we need (2n-2) algebraic equation, which can be provided by selecting (n-1) collocation points and satisfying Eq. (28) at these selected points. In the pseudo-spectral method, the unknown coefficients are obtained by satisfying the differential equations at collocation points. During the use of Chebyshev polynomial as the basis functions, the collocation points are opted based on Chebyshev-Gauss-Lobatto Grid for achieving the minimum error:

$$x_i = \cos\left(\frac{\pi i}{n-2}\right) \qquad i = 0, 1, 2, \ldots, n-2 \qquad (30)$$

In case of mechanical loading, the buckling dimensionless parameter λ is determined using the following relation:

$$\lambda = \frac{P_{cr} b^2}{D_0}$$
(31)

where

$$D_0 = \frac{E_m h_0^3}{12\left(1-\nu^2\right)}$$

3. Numerical Results and Discussion

This section presents the numerical results for buckling analysis of variable thickness circular plates which are made of bimorph FGMs. As shown in Fig. 3, the considered circular plates are either simply supported or clamped, and subjected to radial uniform compression. It is assumed that the thickness variation is in two different forms, including linear and parabolic. Since the buckling analysis of bimorph FGMs circular plates with variable

thickness has not been studied yet, similar results are not available to compare our present results with them. Hence, in order to validate the derived equations and solution method, the problem was initially solved for homogeneous plates with variable thickness. After the certainty of the accuracy of the equations and employed solution method, the buckling behaviors of the circular plates with variable thickness made of bimorph FGMs were evaluated and the obtained numerical results were presented and discussed.

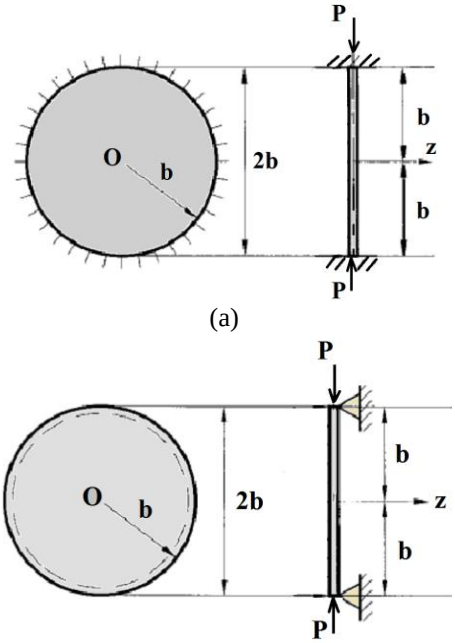

Fig. 3: Boundary conditions of the circular FGM plate: (a) clamped; (b) simply supported

4.1 Homogeneous plates

As determination of the pre-buckling mode under distributed loading in radial direction is a prerequisite for solving the stability equations, firstly, the accuracy of the proposed formulation had to be appraised by solving the membrane equation for pre-buckling load. The obtained results were compared with the results obtained by Wang et al. [31]. Wang and colleagues derived the Plates' equations based on Mindlin theory and used Rayleigh-Ritz method for solving the corresponding differential equations. Note that the results of Wang and colleagues are presented in terms of the stress function *f*. The following relation can be defined between the stress function f and pre-buckling force N_{r0}:

$$f = r N_{r0} \tag{32}$$

The variations of dimensionless stress function $\bar{f}$ with respect to the dimensionless radial coordinate *r/b* are depicted in Fig. 4. In this figure, various values are considered for the taper parameter Ω. Note that the dimensionless stress function $\bar{f}$ is defined as:

$$\bar{f} = \frac{f}{b\,N_{r0}(b)} = \frac{r\,N_{r0}}{b\,P} \tag{33}$$

It is worth to be noted that the taper parameter Ω=0.5 represents a plate with constant thickness. In this case, the dimensionless stress function will alter in a linear manner with respect to the radial direction. It is evident from Fig. 4, that the present results are in good agreement with the results reported by Wang et al. [31].

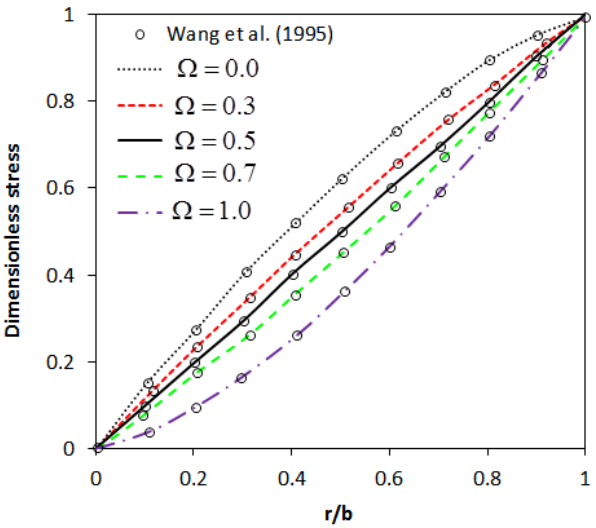

(a)

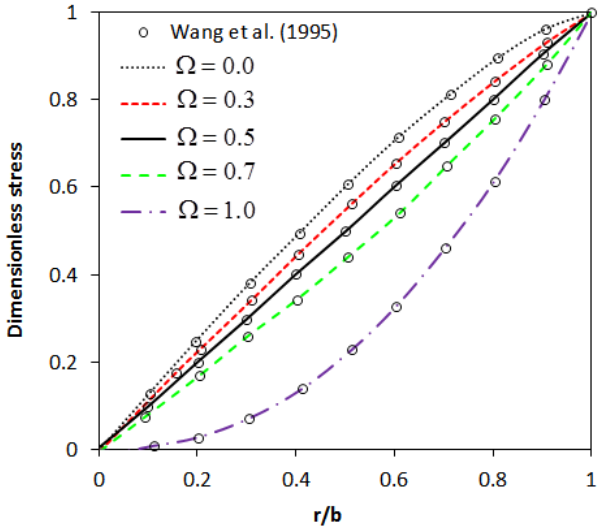

(b)

Fig. 4: Variations of dimensionless stress function against dimensionless radial coordinate for different values of the taper parameter Ω: (a) linear thickness variation; (b) parabolic thickness variation

It can be also inferred from the depicted curves of Fig. 4 that the variations of $\bar{f}$ for high taper parameters such as Ω=1 show considerable deviation from corresponding values for the plate with constant thickness (i.e. Ω = 0.5). Thus, high errors may occur if a constant stress distribution is considered for highly tapered circular plates.

For validating the stability results obtained by utilizing pseudo-spectral method, the buckling analysis of a homogeneous circular plate with constant thickness was also investigated. The obtained results are compared with the results of Wang et al. [32] using Rayleigh-Ritz method, Rajo and Rao [33] using finite element method, Ozakca et al. [9] by utilizing finite element method, and Eskandari-Jam et al. [34] using analytical solution. The results of these comparisons are tabulated in Table 1. It can be observed that the presented method is highly accurate.

With regard to the results of Table 1, it can be stated that the buckling parameter reduces when the plate side ratio h_0/b increases. The main reason for this phenomenon is the shear deformation effect. By increasing h_0/b, the shear deformation effect in the circular plate increases significantly. Such an outcome cannot be observed in the results of Eskandari-Jam et el. [34] which is based on the classical Kirchhoff plate theory. Indeed, the classical Kirchhoff plate theory estimates the value of critical buckling compression more than its real value, and as the thickness increases, such error becomes more evident.

After investigating the accuracy of the present model for the stability analysis of circular plates with constant thickness, the buckling analysis of circular plates with variable thickness was also examined. The results for the plates with simply supported and clamped edges are depicted in Figs. 5 and 6, respectively. In these figures, two different patterns are considered for the thickness variation of the plate: linear and parabolic pattern. The results are presented for various values of side ratio h_0/b. The results of the present research with side ratio h_0/b =0.001 are comparable with the results reported by Wang et al. [31].

Table 1. Comparison study of the buckling parameter λ for homogenous circular plates with constant thickness

Boundary condition		h_0/b				
		0.001	0.01	0.05	0.1	0.2
Clamped	Present	14.6819	14.6758	14.5296	14.0909	12.5724
	Wang et al. [32]	14.6819	14.6759	14.5296	14.0909	12.5725
	Raju and Rao [33]	14.6825	-	14.5299	14.0910	12.5725
	Ozakca et al. [9]	14.6819	14.6746	14.5014	13.9885	12.2843
	Eskandari Jam et al. [34]	14.6819	14.6819	14.6819	14.6819	14.6819
Simply supported	Present	4.1978	4.1973	4.1852	4.1480	4.0056
	Wang et al. [32]	4.1978	4.1973	4.1853	4.1480	4.0056
	Raju and Rao [33]	4.1978	-	4.1852	4.1481	4.0056
	Ozakca et al. [9]	4.1978	4.1972	4.1844	4.1448	3.9938
	Eskandari Jam et al. [34]	4.1978	4.1978	4.1978	4.1978	4.1978

It is seen that the agreement between present results and those results reported by Wang et al. [31] is outstanding. It can also be deduced from these depicted results that by increasing the side ratio, the buckling parameter of the plate decreases due to the shear deformation effect.

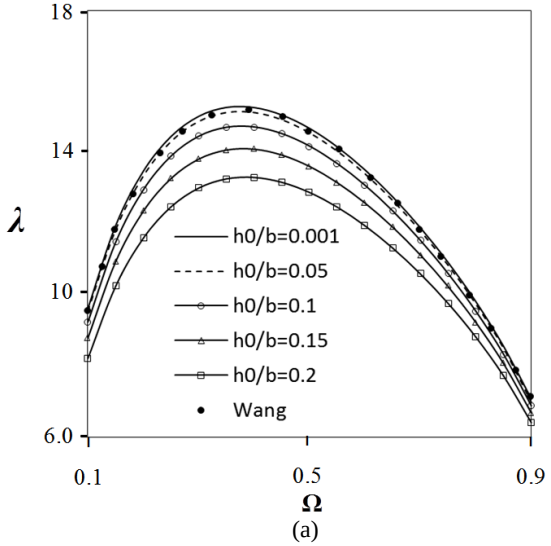

(a)

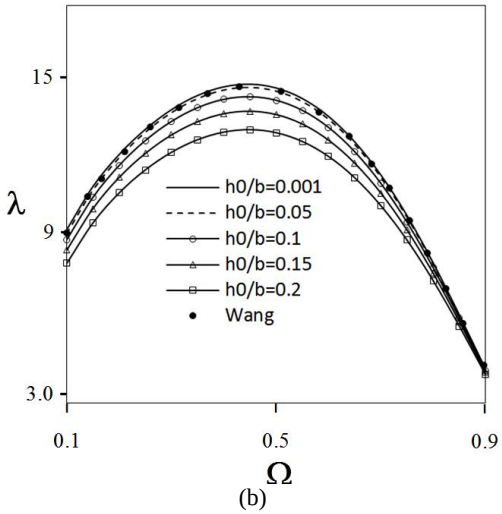

(b)

Fig. 5: Buckling load factor λ with respect to the taper parameter Ω for the clamped plates: (a) linear taper; (b) parabolic taper

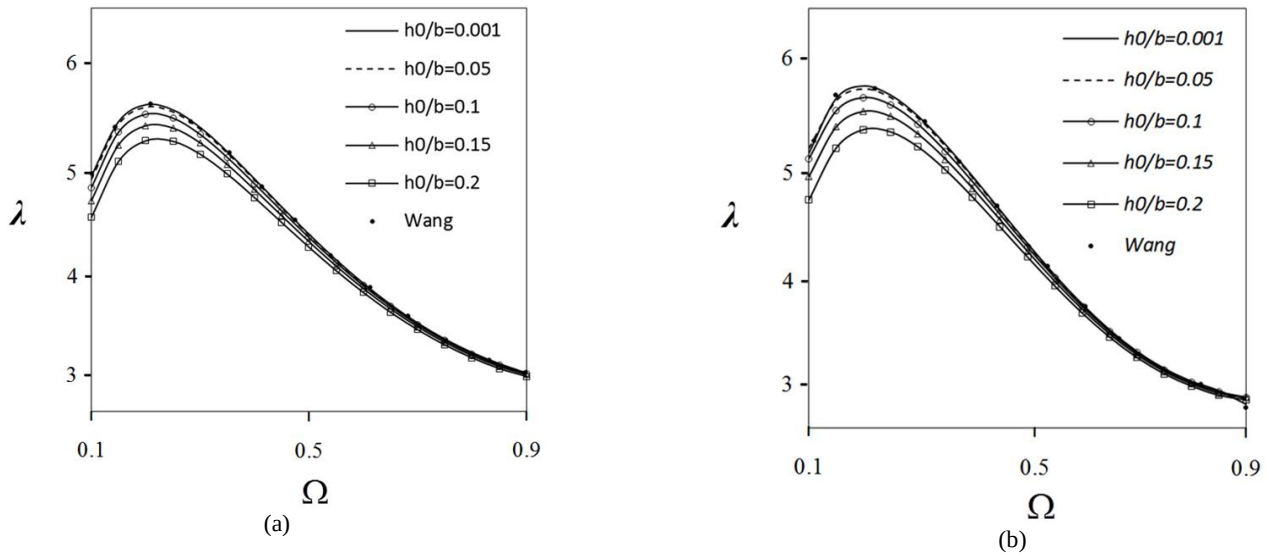

Fig. 6: Buckling load factor λ with respect to the taper parameter Ω for simply supported plates: (a) linear taper; (b) parabolic taper

Table 2. Optimal values of the taper parameter Ω and the corresponding buckling load factor λ for homogenous circular plates

			Wang et al. [31]	Present				
			h_0/b	h_0/b				
Boundary condition	Thickness variations		0.001	0.001	0.05	0.1	0.15	0.2
Clamped	Linear	Ω_{opt}	0.374	0.374	0.374	0.377	0.382	0.387
		λ_{opt}	15.2973	15.2978	15.1283	14.6417	13.8975	12.9755
	Parabolic	Ω_{opt}	0.446	0.447	0.447	0.447	0.447	0.448
		λ_{opt}	14.8335	14.8337	14.6787	14.2325	13.5462	12.6893
Simply supported	Linear	Ω_{opt}	0.210	0.210	0.210	0.214	0.218	0.225
		λ_{opt}	5.8082	5.8062	5.7717	5.6694	5.5080	5.2994
	Parabolic	Ω_{opt}	0.197	0.198	0.199	0.204	0.211	0.220
		λ_{opt}	6.0807	6.0894	6.0312	5.9090	5.7187	5.4766

By observing Figs. 5 and 6, it can be deduced that there is an optimal value for the taper parameter Ω, wherein the value of buckling parameter λ is maximum. The optimal taper parameter Ω as well as the corresponding buckling parameter λ are presented in Table 2 for different values of the side ratio h_0/b. In this table, the optimal values obtained by Wang et al. [31] are also shown. Note that the results of the present research with side ratio h_0/b=0.001 are comparable with the results of reference [31]. As stated previously, the difference between Kirchhoff (classic) plate theory and Mindlin (first-order) shear deformation plate theory increases when the side ratio of the plate increases.

4.2 Bimorph FGM Plates

In this section, the buckling behavior of bimorph FGM circular plates with variable thickness under uniform radial compression is assessed and the numerical results are presented. The assumed FGMs of the present example is a combination of Aluminum (Al), as the metal and Zirconia (ZrO2), as the ceramic. The mechanical properties of Aluminum and Zirconia are presented in Table 3.

Table 3. Properties of FGM ingredients

Material	Modulus of Elasticity (Gpa)	Poisson's ratio
Aluminum	70	0.333
Zirconia	151	0.3

Figs. 7-10 illustrate the relation between buckling parameter λ and the volume fraction index *N* for various values of the taper parameter Ω. The depicted graphs of Figs. 7 and 8 are corresponding to the clamped plates while the graphs of Figs. 9 and 10 are corresponding to the simply supported plates. The side ratio of the plates is assumed to be h_0/b=0.06. Both the linear and parabolic patterns are assumed for the thickness variation of the plates. It is observed that by increasing the volume fraction index, the buckling parameter of the plate increases. Such increase and changes are due to the fact that, as the volume fraction index increases, the ceramic content of the plate increases. Since the stiffness of the ceramic is higher than metal, the total stiffness of the

plate will increase and the resistance of plate against the buckling will increase consequently. It was noticed that as the volume fraction index increases, the buckling parameter increases in a very fast pace. However, this trend for the volume fraction index with values higher than 5 is much lower.

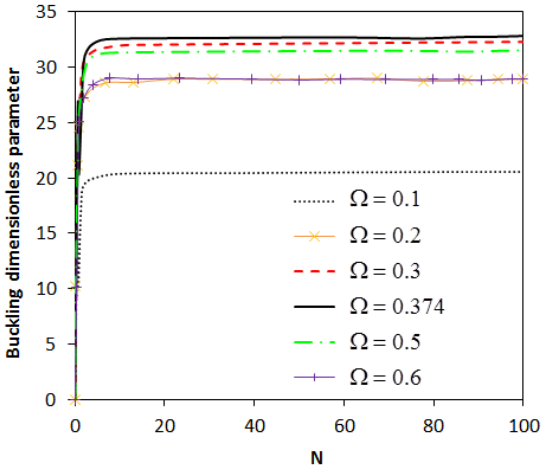

Fig. 7: Variations of the buckling parameter with respect to the volume fraction index for different values of taper parameter-clamped plates with linear variations of thickness

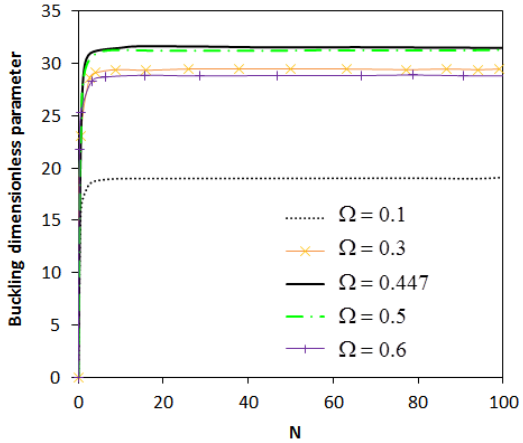

Fig. 8: Variations of the buckling parameter with respect to the volume fraction index for different values of taper parameter-clamped plates with parabolic variations of thickness

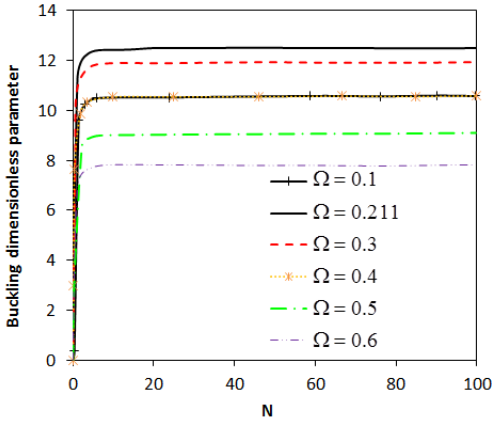

Fig. 9: Variations of the buckling parameter with respect to the volume fraction index for different values of taper parameter-simply supported plates with linear variations of thickness

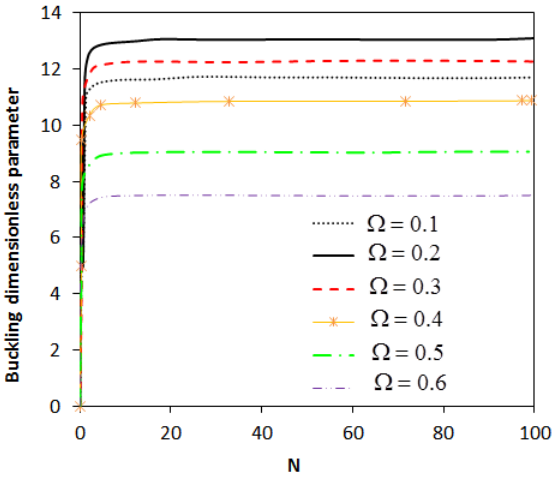

Fig. 10: Variations of the buckling parameter with respect to the volume fraction index for different values of taper parameter-simply supported plates with parabolic variations of thickness

It is evident from Fig. 7 that when the taper parameter increases from 0.1 to 0.374, the buckling parameter increases. However, the buckling parameter decreases as the taper parameter increases from 0.374 to 0.6. The maximum value of the buckling parameter for the clamped bimorph FGMs plate with linear thickness variation is achieved when Ω is equals to 0.374 and the volume fraction index is higher than 5. Regarding Fig. 8, as the taper parameter increases from 0.1 to 0.447, the buckling parameter increases. On the other hand, the buckling parameter λ decreases when the taper parameter Ω increases from 0.447 to 0.6. The maximum value of the buckling parameter for the clamped bimorph FGMs plate with parabolic thickness variation is achieved when Ω is equals to 0.45 and the volume fraction index is higher than 5.

It is evident from Fig. 9 that when the taper parameter increases from 0.1 to 0.211, the buckling parameter increases. However, the buckling parameter decreases as the taper parameter increases from 0.211 to 0.6. For the taper parameters Ω=0.4, Ω=0.1, the buckling parameters are approximately the same. The maximum value of the buckling parameter for the simply supported bimorph FGMs plate with linear variation of thickness is achieved when Ω is equal to 0.211 and the volume fraction index is higher than 5. Concerning the Fig. 10, as the taper parameter increases from 0.1 to 0.2, the buckling parameter increases. On the other hand, the buckling parameter λ decreases when the taper parameter Ω increases from 0.2 to 0.6. The maximum value of the buckling parameter for the simply supported bimorph FGMs plate with linear thickness variation is achieved when Ω is equal to 0.2 and the volume fraction index is higher than 5.

Variations of the buckling parameter λ against the volume fraction index *N* is shown in Figs. 11-12 for various values of the side ratio h_0/b. The results are presented for the bimorph FGM plates with Ω=0.5. The depicted graphs of Fig. 11 are corresponding to the clamped plates while the graphs of Fig. 12 are corresponding to the simply supported plates. It can be

observed from these figures that the buckling parameter of the plate decreases as the side ratio h_0/b increases. It can also be seen that the increase of the volume fraction index from 0 to 5 leads to the considerable increase of the buckling parameter. By increasing the volume fraction index more than 5, the buckling parameter of the plate approaches the buckling capacity of a fully ceramic plate.

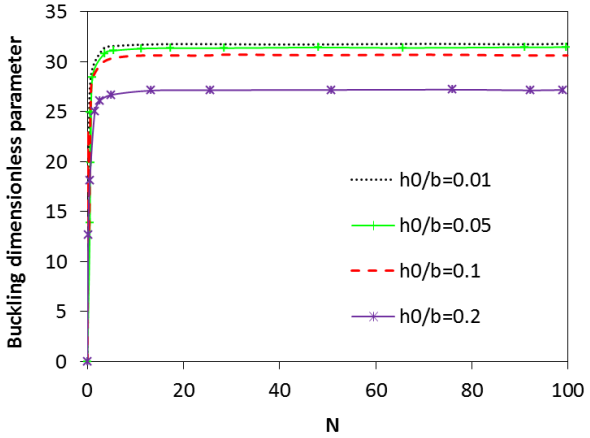

Fig. 11: Variations of the buckling parameter against the volume fraction index for different values of the side ratio - clamped plates

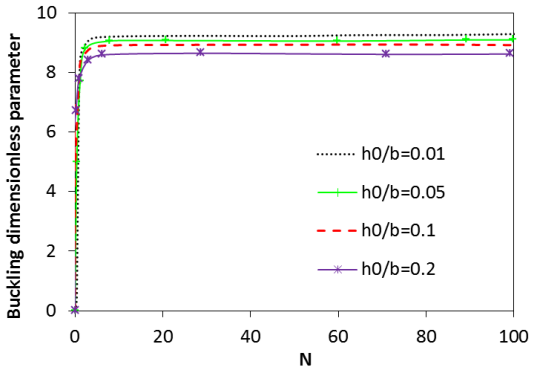

Fig. 12: Variations of the buckling parameter against the volume fraction index for different values of the side ratio - simply supported plates

5. Conclusions

In the present study, the buckling behavior of circular bimorph FGM plates with variable thickness under mechanical loading was investigated. To reach this aim, von Karman's assumptions for geometric nonlinear strains as well as the first-order shear deformation plate theory were employed. A uniform radial form was assumed for the applied compressive load. Moreover, two types of variable thickness FGM plates as well as their fabrication processes were suggested. Except for the Poisson's ratio, all other materials properties of the plate are assumed to be symmetric about its mid-plane. The middle plane and the outside plane of the FGMs plate are assumed to be made of pure metal and pure ceramic, respectively. The material properties change in the thickness direction according to the power law. Shooting method was used for solving the membrane equation. This equation is required for determining the distributions of the pre-buckling force in the radial direction. The stability equations were numerically solved using pseudo-spectral method. In order to assess the critical buckling load, Chebyshev polynomials were used as the basis function. The numerical results were presented for both simply supported and clamped plates. Both the linear and parabolic patterns were considered for representing the thickness variations of the FGM plates. As this problem has not been investigated in previous researches, the obtained results for homogenous plates were employed for the validation of the proposed formulation. The comparisons proved the accuracy of the present results. The present research exhibited that the utilization of the pseudo-spectral method based on Chebyshev basis functions is a suitable solution for solving the buckling problem of circular plates with variable thickness. Even for plates with high thickness variations, this method yields converged results. The other main findings of the present research are summarized as follows:

- In order to analyze the buckling of the plates, it is essential to solve the membrane equations for finding the pre-buckling load. In the plates with variable thickness, the membrane equation is a differential equation with variable coefficient, and the best solution strategy is the use of numerical methods. In this paper, the membrane equation was solved using the shooting method. It utilizes the Runge-Kutta fourth order method and Newton-Raphson correction method simultaneously. Considering the high accuracy of the obtained results and the simplicity of the presented method, the use of the shooting method for solving the membrane equation of plates with variable thickness is highly recommended.
- By investigating the effect of the taper parameter on the buckling load of homogeneous plates subjected to uniform radial compression, it was found that there exists an optimal value for the taper parameter **Ω** wherein the buckling load becomes maximum. For both the linear and parabolic thickness variations, the optimal values of the taper parameter and the corresponding buckling loads were presented for the simply support and clamped plates. These values were also compared with those obtained by pervious researches.
- By increasing of the ratio of thickness to lateral dimension (side ratio), the buckling parameter of the bimorph FGM circular plates reduces.
- By increasing of the volume fraction index, the ceramic volume fraction of the plate increases. Since the ceramic is more rigid than metal, the resistance of the plate against the mechanical buckling increases consequently.
- The resistance of clamped bimorph FGM plates against the mechanical buckling is three times the resistance of simply supported ones. Similar results were detected for the plates made of homogenous materials.

References

[1] Koizumi, M., "The concept of FGM, Ceramic Transactions", Functionally Gradient Materials, vol. 3(1), 1993, pp. 3-10.

[2] Lal, R., Ahlawat, N., "Buckling and Vibration of Functionally Graded Non-uniform Circular Plates Resting on Winkler Foundation", Latin American Journal of Solids and Structures, vol. 12, 2015, pp. 2231-2258.

[3] Brayan, G.H., "On the stability of a plane plate under thrust in its own plane with application to the buckling of the side of a ship", In Proceeding of the London Mathematical Society, vol. 22, 1891, pp. 54-67.

[4] Yamaki, N.B., "Buckling of a thin annular plate under uniform compression, Transactions of ASME", Journal of Applied Mechanics, vol. 25, 1958, pp. 267-273.

[5] Timoshenko, S.P., Gere, J.M., "Theory of elastic stability, 2nd Edition", New York, McGraw-Hill, (1961).

[6] Brush, D.O., Almroth, B.O., "Buckling of bars, plates and shells", New York, McGraw-Hill, (1975).

[7] Reddy, J.N., Khdeir, A.A., "Buckling and vibration of laminated composite plate using various plate theories", AIAA J, vol. 27, 1989, pp. 1808-1817.

[8] Kadkhodayan, M., Zhang, L.C., Sowerby, R., "Analyses of wrinkling and buckling of elastic plates by DXDR method", Computers and Structures, vol. 65(4), 1997, pp. 561-574.

[9] Ozakca, M., Taysi, N., Kolcu, F., "Buckling analysis and shape optimization of elastic variable thickness circular and annular plates-I. Finite element formulation", Engineering Structures, vol. 25, 2003, pp. 181-192.

[10] Xu, R.Q., Wang, Y., Chen, W.Q.,"Axisymetric buckling of transversely isotropic circular and annular plates", Arch Appl Mech, vol. 74, 2005, pp. 692-703.

[11] Najafizadeh, M.M., Eslami, M.R., "First-order-theory-based thermoelastic stability of functionally graded material circular plates", AIAA J, vol. 40, 2002, pp. 1444-1450.

[12] Najafizadeh, M.M., Eslami, M.R., "Buckling analysis of circular plates of functionally graded materials under uniform radial compression", International Journal of Mechanical Sciences, vol. 44, 2002, pp. 2479-2493.

[13] Naei, M.H., Masoumi, A., Shamekhi, A., "Buckling analysis of circular functionally graded material plate having variable thickness under uniform compression by finite-element method", Proceeding Institution Mech. Eng. Part C, J. Mech Eng. Sci, vol. 221, 2007, pp. 1241-1247.

[14] Sepahi, O., Forouzan, M.R., Malekzadeh, P., "Thermal Buckling and post buckling analysis of functionally graded annular plates with temperature-dependent material properties", Materials and Design, vol. 32, 2011, pp. 4030-4041.

[15] Golmakani, M.E., Emami, M., "Nonlinear bending and buckling analysis of functionally graded annular plates", Modares Mechanical Engineering, vol. 13(11), 2013, pp. 1-14.

[16] Khosravi, H., Khosravi, M., Khosravi, M., Shoaib Mousavi, S., "Analyzing thermal stability of circular plates made of FGM bimorphs considering the first-order shear deformation theory", Indian Journal of Science and Technology, vol. 8(12), 2015, pp. 53110.

[17] Khosravi, H., Khosravi, M., "An exact solution of thermal stability analysis of bimorph functionally graded annular plates", Revista de la Construcción, vol. 16(1), 2017, pp. 66-81.

[18] Lezgy-Nazargah, M., Vidal, p., Polit. O., "An efficient finite element model for static and dynamic analyses of functionally graded piezoelectric beams", Composite Structures, vol. 104, 2013, pp. 71-84.

[19] Lezgy-Nazargah, M., Farahbakhsh, M., "Optimum material gradient composition for the functionally graded piezoelectric beams", International Journal of Engineering, Science and Technology, vol. 5(4), 2013, pp. 80-99.

[20] Lezgy-Nazargah, M., "A three-dimensional exact state-space solution for cylindrical bending of continuously non-homogenous piezoelectric laminated plates with arbitrary gradient composition", Archive of Mechanics, vol. 67(1), 2015, pp. 25-51.

[21] Lezgy-Nazargah, M., "A three-dimensional Peano series solution for the vibration of functionally graded piezoelectric laminates in cylindrical bending", Scientia Iranica, vol. 23(3), 2016, pp. 788-801.

[22] Lezgy-Nazargah, M., "Fully coupled thermo-mechanical analysis of bi-directional FGM beams using NURBS isogeometric finite element approach", Aerospace Science and Technology, vol. 45, 2015, pp. 154–164.

[23] Lezgy-Nazargah, M., Meshkani, Z., "An efficient partial mixed finite element model for static and free vibration analyses of FGM plates rested on two-parameter elastic foundations", Structural Engineering and Mechanics, vol. 66(5), 2018, pp. 665-676.

[24] Baferani, A.H., Saidi, A.R., Ehteshami, H., "On free vibration of functionally graded mindlin plate and effect of in-plane displacements", Journal of Mechanics, vol. 29(2), 2013, pp. 373-384.

[25] Soltani, M., "Vibration characteristics of axially loaded tapered Timoshenko beams made of functionally graded materials by the power series method", Numerical Methods in Civil Engineering, vol. 2(1), 2017, pp. 1-14.

[26] Soltani, M. and Mohri, F., "Stability and vibration analyses of tapered columns resting on one or two-parameter elastic foundations", Numerical Methods in Civil Engineering, vol. 1(2), 2014, pp. 57-66.

[27] Soltani, M. and Sistani, A., "Elastic stability of columns with variable flexural rigidity under arbitrary axial load using the finite difference method", Numerical Methods in Civil Engineering, vol. 1(4), 2017, 23-31

[28] Soltani, M., Asgarian, B., "Determination of lateral-torsional buckling load of simply supported prismatic thin-walled beams with mono-symmetric cross-sections using the finite difference method", Amirkabir Journal of Civil Engineering, vol. 50(1), 2018, 23-26.

[29] Soltani, M. and Asgarian, B., "Buckling analysis of axially functionally graded columns with exponentially varying cross-section", Modares Civil Engineering Journal, vol. 18(3), 2018, pp. 87-97.

[30] Boyd, J.P., "Chebyshev and Fourier Spectral Methods", New York, Dover, (2000).

[31] Wang, C.M., Hong, G.M., Tan, T.J., "Elastic buckling of tapered circular plates", Computers & Structures, vol. 55, 1995, pp. 1055-1061.

[32] Wang, C.M., Xiang, Y., Kitipornchai, S., Liew, K.M., "Axisymmetric buckling of circular Mindlin plates with ring supports", Journal of Structural Engineering, vol. 119, 1993, pp. 782–793.

[33] Raju, K.K., Rao, G.V., "Finite element analysis of post-buckling behavior of cylindrical orthotropic circular plates", Fibre Science and Technology, vol. 19, 1983, pp. 145–154.

[34] Eskandari-Jam, J., Khosravi, M., Namdaran, N., "An exact solution of mechanical buckling for functionally graded material bimorph circular plates", Metallurgical and Materials Engineering, vol. 19(1), 2013, pp. 45-63.